# ASSESSMENT OF TWO DISCRETIZATION STRATEGIES TO SIMULATE THE COMPRESSION CYCLE OF RECIPROCATING COMPRESSORS

**Leíza R Silva, leiza.reis@polo.ufsc.br**
**César J Deschamps, deschamps@polo.ufsc.br**
POLO Research Laboratories, Federal University of Santa Catarina, Florianópolis, SC, Brazil

**Tadeu T Rodrigues, tadeu.t.rodrigues@embraco.com**
**Evandro L L Pereira, evandro.l.lange@embraco.com**
Embraco – Research and Development, Rua Ruy Barbosa, Joinville, SC, Brazil

***Abstract.*** *CFD models have been widely employed to predict fluid flow and heat transfer inside the compression chamber of reciprocating compressors due to the importance of such phenomena in the compressor efficiency. This paper presents a comparative analysis between two different discretization approaches to simulate the compression cycle, a Dynamic Mesh (DM) and an Automatic Mesh Refinement (AMR). The simulation model adopts a transient three-dimensional formulation and considers a moving piston with specified displacement and ideal automatic valves for the suction and discharge processes. In the DM model the volumes are stretched or compressed during the piston displacement, always maintaining the same number of total volumes. On the other hand, the mesh in the AMR model is generated for each position of the piston and new volumes can be created according to specified parameters. Despite the much larger use of RAM memory by the AMR model, its computational cost was found to be significantly smaller than that of the DM model.*

***Keywords****: Compression Cycle, Dynamic Mesh, Automatic Mesh Refinement*

## 1. INTRODUCTION

Refrigeration systems are responsible for a large amount of the electrical energy consumption. Therefore, efficiency improvement of such systems can offer great energy savings in domestic and industrial applications. Among the technologies employed to refrigerate products or environment, the vapor compression refrigeration cycle is the most widespread. Household refrigerators work based on this type of refrigeration cycle and employ reciprocating compressors, which are the main component of the system when it comes to energy consumption. For this reason, studies on the performance of reciprocating compressors are important to improve the efficiency of the whole system.

The electrical and mechanical efficiencies of reciprocating compressors have been extensively studied during the last decades. Most of the studies aiming at improving the global performance of the compressor are focused on its compressible cycle, and therefore models to predict heat transfer and fluid flow inside the compressor are very important. In reciprocating compressors, heat transfer and fluid is investigated employing models of different degrees of complexity, such as lumped, differential (Oliveira *et al.*, 2015) and hybrid approaches (Lohn *et al.*, 2015). Simulation models based on the differential formulation are computationally expensive and, therefore, it is common to be applied only to some components, such as the compression chamber. Transient thermodynamic processes in the compression chamber of reciprocating compressors have been studied both experimentally (Morriesen and Deschamps, 2012), with an investigation of superheating in the suction chamber, and numerically (Pereira *et al.*, 2012), with a simplified model for the suction process. Despite the physical insight provided by measurements, numerical simulation is widely used due to its versatility and the possibility of obtaining the required results in a shorter period of time.

Regarding the simulation models, computational fluid dynamics (CFD) has been extensively employed, with the fluid solution domain being sometimes surrounded by moving boundaries. Dynamic Mesh (DM) approaches have been widely applied in such situations, including problems associated with engine injector flow (Xandra *et al.*, 2010), multiphase flow (Di *et al.*, 2008) and porous media (Duque *et al.*, 2015). On the other hand, the Automatic Mesh Refinement (AMR) approach is widely adopted in transient simulations of engine spray, as presented by Li and Kong (2009). The main difference between the DM and AMR approaches is that a new mesh is created at run-time during the simulation in the AMR, while in the DM model the total number of volumes is kept constant, with the volumes being extended or stretched depending on the movement of boundaries.

This paper presents a comparative analysis of two mesh models to simulate the compression cycle of a reciprocating compressor designed for household refrigeration. The analysis takes into account meshing approaches, the Dynamic Mesh and the Automatic Mesh Refinement, considering the solution methods and accuracy.

## 2. GEOMETRY AND BOUNDARY CONDITIONS

The geometry used in the simulations represents the compression chamber of a reciprocating compressor applied in household refrigeration, operating with R-600a. The compressor speed was set to 2000 rpm, with the following suction and discharge conditions: ($T_s$= 50°C, $p_s$ = 0.58kPa) and ($T_d$ = 120°C, $p_d$ = 5.28kPa).

Figure 1 shows the geometry of the compression chamber after some simplifications, such as the removal of suction and discharge reed valves. The cylinder diameter was set to 24 mm, the piston stroke to 17.6 mm and the orifice height (h*) of the suction and discharge orifices to 1.3 mm. Due to the motion of the piston, the mesh must be modified during the simulation to correctly characterize the compression cycle. The valves were considered ideal and, when opened, allowed the flow through the suction and discharge orifices. The valve opening and closing points were obtained by combining experimental data and theoretical analysis, being defined by the corresponding crankshaft angles $\theta$. Accordingly, the suction valve was set to open at $\theta$=200° and close at $\theta$=360°, whereas the discharge valve opening and closing were set to $\theta$=150° and 180°, respectively.

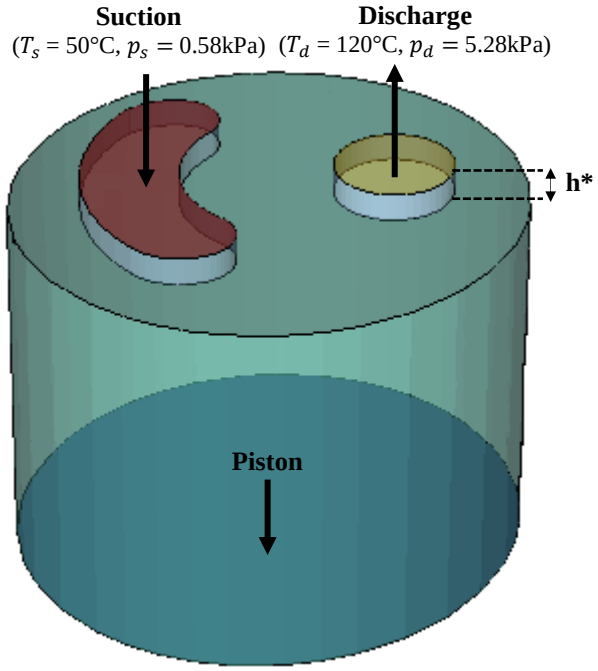


Figure 1. Compressor chamber geometry.

The boundary condition applied to the suction and discharge valves were Newman condition for velocity and Dirichilet condition for pressure. The non-slip flow condition was adopted at the solid walls. The piston displacement ($z_p$) was defined by

$$z_p = e\cos\theta + \sqrt{b^2 - (e\sin\theta - d)^2} - a_p \quad (1)$$

where $\theta$ is the crankshaft angle, i.e.,

$$\theta = (2\pi f)t + \sin^{-1}(d/(b-e)) \quad (2)$$

and $e$ is the eccentricity, $t$ is the time, $b$ is the connecting rod length, $d$ is the wrist pin offset and $a_p$ is an adjustment that can be set to the piston displacement so as to result the correct clearance at top dead center.

## 3. SIMULATION PARAMETERS

### 3.1 Computational Mesh

*3.1.1 Dynamic Mesh (DM)*

Several engineering applications of fluid dynamics employ the Dynamic Mesh approach, particularly for transient simulations. During a simulation with DM, it is possible to change or to maintain fixed the number of mesh nodes. Xandra *et al.* (2010) suggested some strategies for meshing of fluid flow solution domains with moving surfaces, such as: (a) prescribing the mesh movement via defined functions keeping constant the number of nodes, (b) rebuilding the mesh by changing the number of nodes, (c) mesh morphing with set surface movement. In this study, the Dynamic Mesh

followed the piston motion prescribed by Eq. (1) to calculate the 3D mesh displacement. As a result, the volumetric mesh is squeezed or compressed during the simulation without changing the number of nodes.

The commercial code ANSYS-CFX® has default tools to automatically calculate the mesh movement, and therefore further programming was not required. In addition, ANSYS-CFX® offer the alternatives of repositioning all nodes of the mesh or just the nodes of a specific region (Srikanth and Bhasker, 2009). Moreover, the grid displacement can be prescribed either relative to the initial mesh or relative to the mesh of the previous crankshaft angle.

*3.1.2 Adaptive Mesh Refinement (AMR)*

The AMR approach was analyzed through the commercial code Converge®. The AMR automatically creates a local mesh refinement in regions that require higher resolution, eliminating the consuming time of meshing associated with other approaches. In transient simulations, this is performed at run-time by the code. A comparative analysis between automatic mesh refinement and fixed mesh was presented by Xue and Kong (2009) and Li and Kong (2009). The authors of both studies concluded that greater numerical accuracy is achieved when the AMR was used for spray modeling.

In the AMR approach available in the code Converge®, the mesh is defined from a base grid size in which the number of nodes is always smaller than the maximum nodes defined in the automatic refinement. The maximum embedding level define the number of times that the base grid is split. Figure 2 shows a mesh partition with three levels of refinement, where N0 corresponds to the base grid and N3 is the mesh with the highest number of elements, whose cells are eight times smaller than the single cell of the base grid (N0).

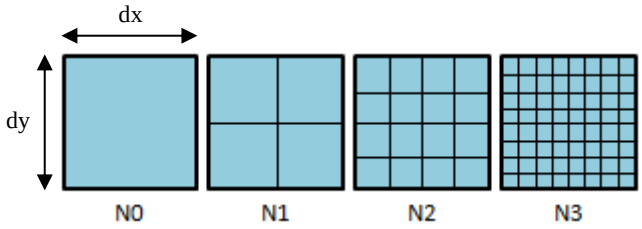


Figure 2. Mesh partition from base grid (N0) to three levels of refinement in AMR mesh.

The mesh is automatically refined based on the parameters specified by the user. To this extent, variables must be chosen to manage the mesh refinement during run-time. In the present study, velocity and temperature were used for this purpose, since they depend on the maximum embedding level and sub-grid criterion, which are calculated from the base grid size.

The sub-grid criterion delimitates a value between 0.1% and 10% of the velocity in the solution domain, above which there will be automatic mesh refinement. The total number of mesh volumes (cells) is calculated permanently during simulation until reach the maximum mesh volumes ($3 \times 10^5$). However, as the mesh refinement is based on the parameters specified by the user, if the number of cells exceeds the pre-defined maximum number of volumes during the meshing, the sub-grid criterion will be increased automatically in order to respect the maximum number of cells. Therefore, once the maximum number of cells is set, there is a limit for the sub-grid criterion, bellow that the criterion specified by user won't be respected.

The required refinement levels were assessed before the comparative analysis between the two meshing approaches. The best results were obtained with three maximum embedding level and 1.0 as sub grid-criterion of velocity.

### 3.2 Turbulence Modeling

In both meshing approaches, the RNG $k$-$\varepsilon$ turbulence model was used to calculate the turbulent transport of the flow inside the compression chamber. The Dynamic Mesh and Adaptive Mesh Refinement methods use the wall-functions proposed Launder and Spalding (1974). However, the turbulence modeling approach employed by both methods presents a small difference in terms of wall functions (ANSYS, 2015; Converge, 2016). The wall-function is used in cases where low cell resolution is encountered near the wall. In this case, these functions are able to connect the wall and the log region where the first cell centroid is located. The ANSYS-CFX® software uses *Scalable Functions* as an extension of the method in order to improve the wall-functions in the logarithmic region, while Converge® uses the default wall functions.

### 3.3 Solution method

The differential equations are integrated and solved through the finite volume method (FVM) via segregated or coupled solution procedures. For the DM approach, we selected the coupled solution procedure in which the momentum and pressure equations are solved simultaneously (ANSYS, 2015). On the other hand, the segregated procedure was employed for the AMR approach, with the pressure-velocity coupling being carried out through a modified Pressure Implicit with Splitting of Operators (PISO) algorithm. This method solves the momentum equations and the pressure equation sequentially (Converge, 2016).

The simulation models with both meshing approaches (DM and AMR) adopt the Rhie-Chow interpolation scheme for the velocity field (ANSYS, 2015; Converge, 2016). The Rhie-Chow algorithm is a non-linear interpolation scheme used to avoid the decoupling of flow properties between adjacent cells. The second order backward Euler algorithm was used to solve the transient fluid flow.

### 3.4 Initial Flow Condition

The simulation starts with the piston at top dead center (TDC) in the DM approach and with the piston at bottom dead center (BDC) when the AMR approach is used. The initial pressure and temperature of the gas inside the cylinder are prescribed with reference to the operating condition, i.e., suction pressure and temperature ($p_s$ and $T_s$) for AMR and discharge pressure and temperature ($p_d$ and $T_d$) for DM.

## 4. RESULTS

As already mentioned, the suction and discharge processes were simulated considering ideal valves. Hence, between their corresponding opening and closing crankshaft angles, the valves allow the flow of refrigerant through their orifices. Both meshing approaches present a structured mesh with orthogonal volumes, as shown in Figure 3. An analysis of mesh refinement was conducted for the DM to ensure the independence of the mesh with respect to the monitored variables (pressure, mass flow and piston velocity). The initial number of volumes was approximately equal to 6000 in both simulation models. A fixed time-step of 2 x $10^{-5}$s was used for DM, while a variable time-step between 5 x $10^{-5}$s and 1 x $10^{-7}$s was set for AMR model.

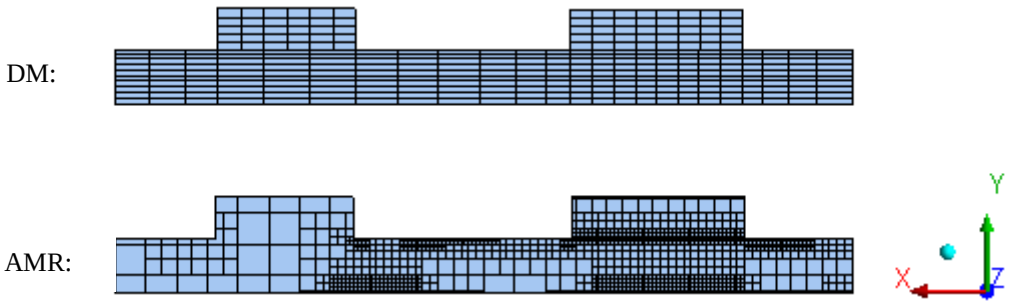


Figure 3. Schematics of meshes of the DM and AMR approaches.

Figure 4 shows the mass of refrigerant in the compression chamber during the suction and discharge processes. As can be seen, the fully cyclic operating condition is reached after two cycles with both models. Convergence of the solution procedure was verified by monitoring the difference between the amount of mass suctioned and the amount of mass discharged in the suction and discharge valves in each compression cycle. Figure 4 also shows that both models predict very similar amount of refrigerant inside the compression chamber throughout the cycle, although slightly less mass is observed at top dead center for the AMR approach. In fact, this difference is around 1.2%.

Figure 5 presents results for the average pressure inside the compression chamber obtained with both models. The pressure was normalized by the suction pressure ($p_s$) in both models. Some discrepancies are observed between the predictions, especially in the discharge process, when the piston is closer to the top dead center. Such discrepancies are seen throughout the cycles.

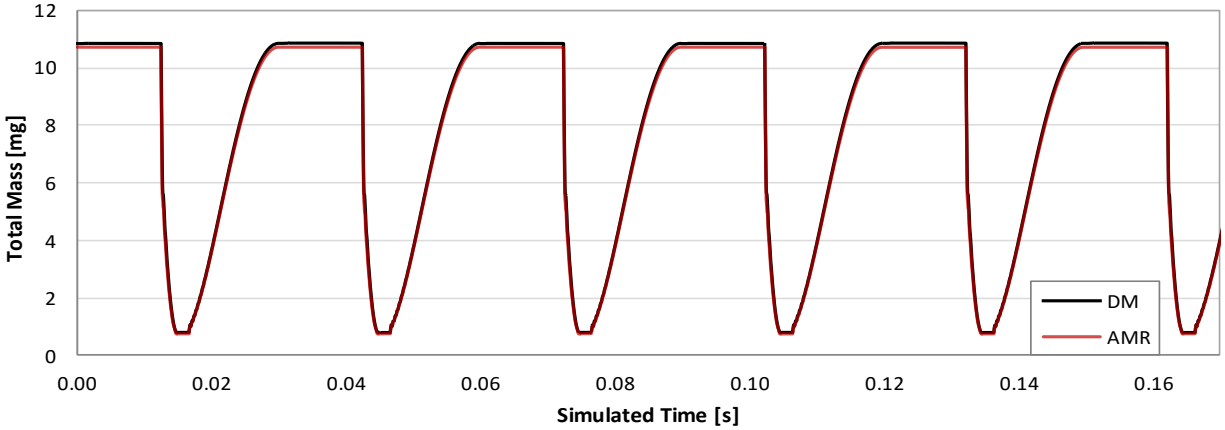


Figure 4. Total mass in the compression chamber during six the compression cycles.

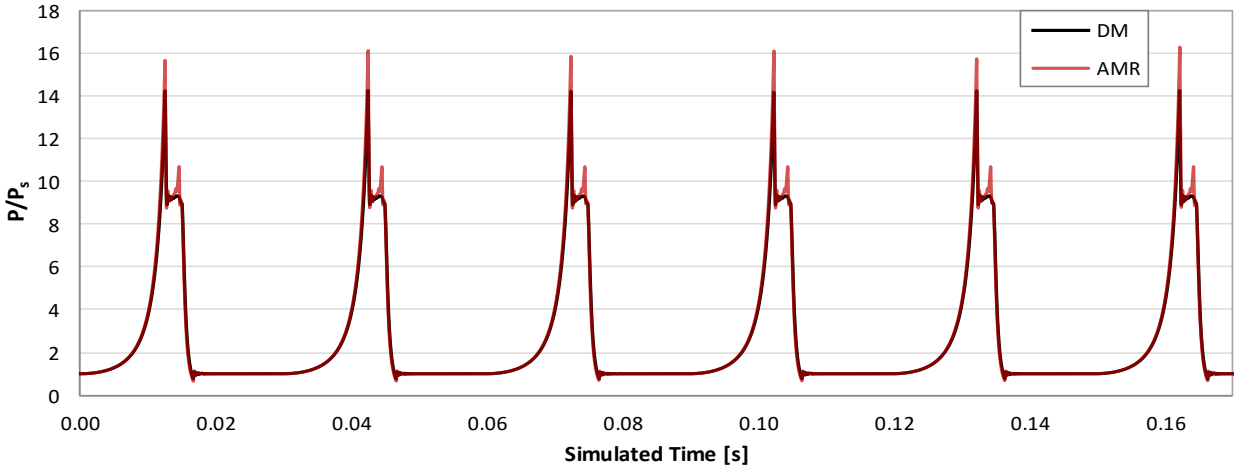


Figure 5. Dimensionless pressure in the cylinder during six the compression cycles.

Figure 6a presents the comparison between results for the average pressure obtained with the DM and AMR models for a single compression cycle, where the inferior limit (grey line) corresponds to normalized suction pressure and the superior limit (grey line) corresponds to normalized discharge pressure. The agreement between the models can be considered satisfactory at the beginning of the compression process, with both curves showing the same rate of pressure increase. However, after the crankshaft angle of 100°, the increase of pressure predicted by the AMR model is higher than that of the DM model. It is clear that the most significant discrepancies between the models are occur at the pressure peak immediately before the opening of the discharge valve ($\theta$ = 150°) and near the end of the discharge process ($\theta$=180°). Otherwise, the curves from both models are in close agreement with one another during the expansion process (180° < $\theta$ < 200°) and also during the entire suction process (200° < $\theta$ < 360°), as can be observed in Fig. 6a. The Pressure-Volume diagram is shown in Fig. 6b, the diagram integration reveals an indicated power of around 40W, with a difference between the models around 5.4%.

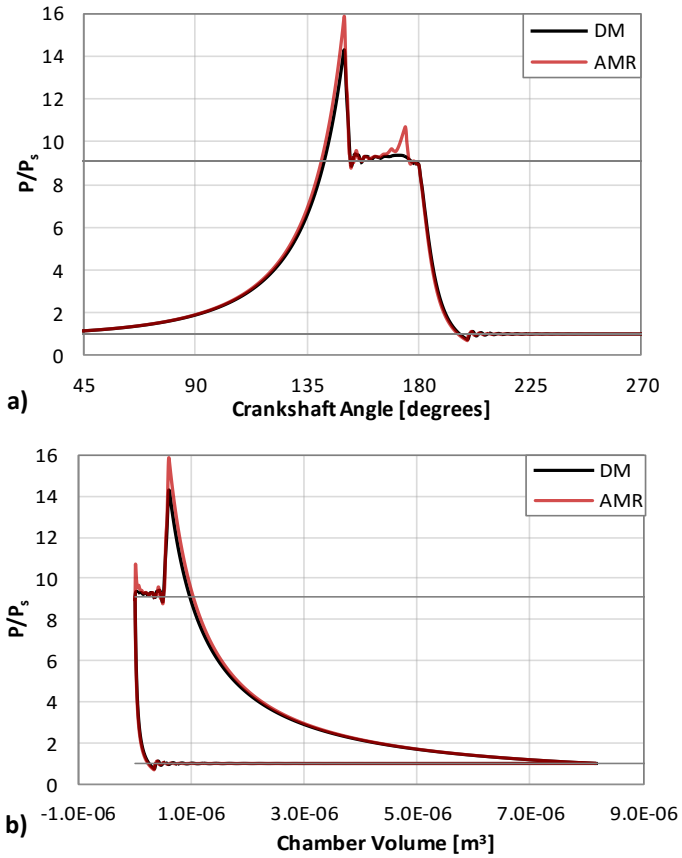


Figure 6. Results for: a) Normalized pressure at cylinder surface during one compression cycle, b) Pressure-Volume diagram with normalized pressure.

The pressure curve predicted by the AMR model shows a second peak of pressure near $\theta$ = 170°, which is not present in the predictions of the DM model (Fig. 6a). As shown in Fig. 7a, the AMR model predicts oscillations in the mass flow rate, with a decrease for crank angles in the interval 170° < $\theta$ < 174° that gives rise to the pressure peak at the same crankshaft angles (Fig. 7b). When the mass flow rate increases again ($\theta$=174°), the pressure is suddenly decreased. The second peak of pressure in the cylinder is strongly influenced by oscillations of mass flow rate through the discharge valve. This phenomenon is particularly strong after $\theta$=170°, when the volume of the compression chamber reaches its minimum and even small oscillations affect the pressure and temperature.

Figure 8 presents results for mass flow rates in the discharge and suction processes obtained with both models under study. The mass flow rates were normalized by the average mass flow at discharge (Figs. 7a and 8a) and at suction (Fig. 8b), respectively. Immediately after the valve opens, at the crankshaft angle 150° the discharge mass flow rate is seen to increase more rapidly in the prediction of the AMR model. This is originated by the pressure peak observed right before the opening of the discharge valve ($\theta$=150°). Otherwise, both models present agreement during the suction process, where there is no peak observed after the opening of the suction valve. Despite the peak of mass flow rate predicted by the AMR model, the integrated mass at the discharge and suction processes are very similar to those obtained with the DM model, with a difference of 3.8% and 0.9% (Figs. 8a and 8b), respectively.

Overall, the agreement between the results of both simulation models is considered satisfactory, especially when one takes into account they were developed with two codes with different solution methods and turbulence models.

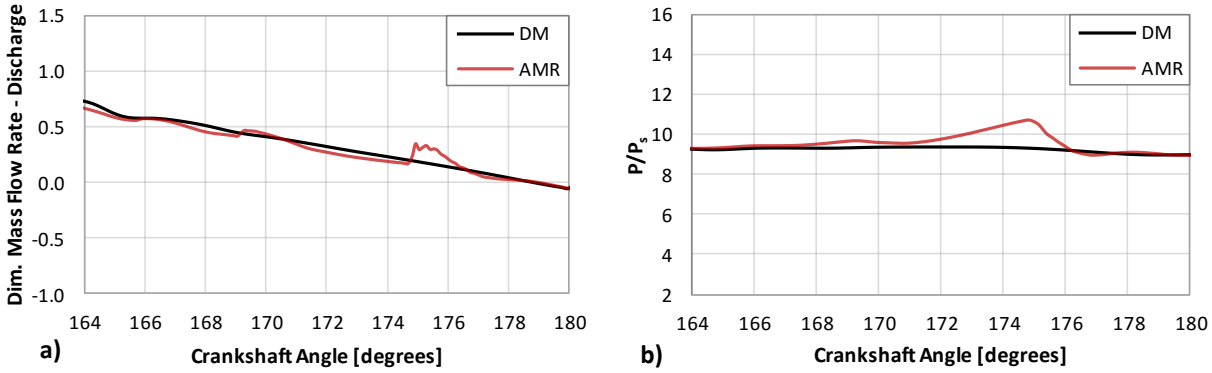


Figure 7. Detailed results for: a) Dimensionless mass flow rate at discharge, b) Dimensionless pressure in cylinder.

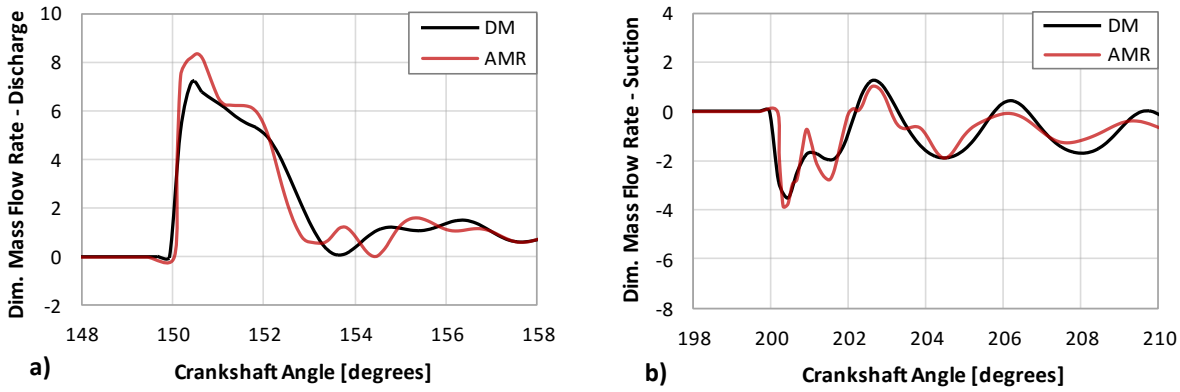


Figure 8. Results for: a) Dimensionless mass flow rate at discharge, b) Dimensionless mass flow rate at suction.

## 5. CONCLUSION

This paper presented a comparative analysis between two meshing approaches adopted to simulate the compression cycle of a reciprocating compressor designed for household refrigeration, represented by the Adaptive Refinement Mesh (AMR) and Dynamic Mesh (DM) methods. The suction and discharge valves were considered ideal and set to open and close at specific crank angles. In order to predict the turbulent flow inside the cylinder, the RNG $k$-$\varepsilon$ turbulence model was used in combination with wall-functions. Overall, the agreement between the results of both models was considered satisfactory. Nevertheless, some discrepancies were observed in the pressure variation immediately before the discharge valve opens and during the expansion process. These aspects will be investigated in further works, with especial attention to the modeling of the valve dynamics.

## 6. ACKNOLEDGEMENTS

The present research has been developed as result of a technical-scientific cooperation program between Federal University of Santa Catarina and EMBRACO. The study was supported by EMBRAPII Unit Polo/UFSC (Brazilian Company of Research and Industrial Innovation).

## 7. REFERENCES

Di, Y., Li, R., and Tang, T., 2008. "A General Moving Mesh Framework in 3D and its Application for Simulating the Mixture of Multi-Phase Flows". Journal of Communication in Computational Physics, Vol. 3, No. 3, pp. 582-602.

Duque, J. C. M., Almeida, R. M. P. and Antontsev, S. N., 2015. "Application of the Moving Mesh Method to the Porous Medium Equation with Variable Exponent". Journal of Mathematics and Computers in Simulation, Vol. 118, pp. 177–185.

Launder, B. and Spalding, D., 1974. "The Numerical Computation of Turbulent Flows". Journal of Computer Methods in Applied Mechanics and Engineering, Vol. 3, pp. 269-289.

Li, Y. and Kong, S.,-C., 2009. "Integration of Parallel Computation and Dynamic Mesh Refinement for Transient Spray Simulation". Journal of Computer Methods in Applied Mechanics and Engineering, Vol. 198, pp. 1596–1608.

Lohn, S. K., Diniz, M. C. and Deschamps, C. J., 2015. "A Thermal Model for Analysis of Hermetic Reciprocating Compressors Under the On-off Cycling Operating Condition". In Proceedings of the 9th International Conference on Compressors and their Systems. London, United Kingdom. Paper no. 12068.

Morriesen, A. and Deschamps, C. J., 2012. "Experimental Investigation of Transient Fluid Flow and Superheating in the Suction Chamber of a Refrigeration Reciprocating Compressor". Journal of Applied Thermal Engineering, Vol. 41, pp. 61–70.

Oliveira, M. J., Diniz, M. C. and Deschamps, C. J., 2015. "Thermal Modeling and Analysis of an Oil-free Compressor Thermal Modeling and Analysis of an Oil-free Linear Compressor". In Proceedings of the 9th International Conference on Compressors and their Systems. London, United Kingdom. Paper no. 012016.

Pereira, E. L. L., Santos, C. J., Deschamps, C. J. and Kremer, R., 2012. "A Simplified CFD Model for Simulation of the Suction Process of Reciprocating Compressors". Proc. International Compressor Engineering Conference at Purdue. West Lafayette, IN, USA. Paper no. 1276.

Srikanth, C. and Bhasker, C., 2009. "Flow Analysis in Valve with Moving Grids Through CFD Techniques". Journal of Advances in Engineering Software, Vol. 40, pp. 193-201.

Xandra, M., Fajardo, P., Patouna, S. and Hoyas, S., 2010. "A Moving Mesh Generation Strategy for Solving an Injection Internal Flow Problem". Journal of Mathematical and Computer Modelling, Vol. 52, pp. 1143–1150.

Xue, Q. and Kong, S.,-C., 2009. "Development of Adaptive Mesh Refinement Scheme for Engine Spray Simulations". Journal of Computers & Fluids, Vol. 38, pp. 939–949.

ANSYS Inc. 2015. Solver Theory Guide. 87 p.

CONVERGE User Manual 2.3. 2016. 100 p.

## 8. RESPONSIBILITY NOTICE

The authors are the only responsible for the printed material included in this paper.